



Monitoring of a secondary recovery application of leachate injection into a heap

Dale F. Rucker ^{a,*}, Michael McNeill ^{a,1}, Al Schindler ^b, Gillian Noonan ^{a,1}

^a hydroGEOPHYSICS, Inc., 2302 N Forbes Blvd, Tucson, AZ 85745, United States

^b Newmont Mining Corp, Gold Quarry Administration, PO Box 669, Carlin, NV 89822, United States

ARTICLE INFO

Article history:

Received 19 June 2009

Received in revised form 17 August 2009

Accepted 31 August 2009

Available online 11 September 2009

Keywords:

Heap leach

Electrical resistivity

Gold production

Geophysics

Monitoring

ABSTRACT

An electrical resistivity monitoring survey was conducted on a mine heap to track fluid movement during high pressure injections. The injections were part of Newmont's patent-pending process called Hydro-Jex, where high pressures and flow rates were used to add significant volumes of fluid within multiple depths or zones. For this experiment, injections occurred in two wells over a seven day period, with a total of about 3000 m³ of leachate added to each well. The resistivity data showed that the flow of leachate can be affected by low permeability zones. The cascading effect of leachate moving along the top of low permeability horizons and finally draining over the edge was directly observed in the resistivity data. Furthermore, it was observed in the resistivity that thin horizons of increasing saturation can travel at least 40 m from the injection well. Lastly, crude approximations to hydrological parameters may be obtained with the data, such as the change in water content, but calibration of the resistivity data with a few moisture sensors would be preferable and likely more reliable.

© 2009 Elsevier B.V. All rights reserved.

1. Introduction

Large engineered earthen structures such as rock piles, heaps, and ore stockpiles are inherently heterogeneous (Lefebvre et al., 2007; Decker and Tyler, 1999; Wu et al., 2007). Dumping practices over the life of the pile's creation will likely have changed, so will have the geological materials encountered within the excavation area, causing properties such as porosity, grain size, and permeability to spatially vary. The variability in hydraulic flow properties will also affect leachate infiltration rates and coverage, and there is a propensity for preferential flow paths to develop (see work by Orr 2002; Orr and Vesselinov, 2002; Wu et al., 2009). The flow paths will cause a significant portion of the leachate to bypass large regions of the heap, making the leaching process less efficient.

Secondary recovery is an effective method to increase the efficiency of a heap. Secondary recovery is defined here as processes used to rework the heap after cessation of the initial leaching cycle. Furthermore, any additional leaching to obtain the residual metal without the reworking would provide marginal gain, as demonstrated through metal recovery (or breakthrough) curves. The marginal gain is due to the preferential flow channels within the heap that readily leach the exposed ore, leaving diffusion-dominating processes at the end of the primary leaching cycle. These processes occur at very long time scales, thus the long tail at the end of the metal recovery curve.

To expose new ore surfaces to leachate and speed the closure of the rock pile, options such as re-contouring of side slopes (Seal and Jung, 2005) and re-ripping surfaces (Uhrie and Koons, 2001) are inexpensive means of secondary recovery. Re-contouring and re-ripping tend to homogenize the top lift. Irrigation of the reworked surfaces may influence new leachate pathways, but it is likely that some deep established flow paths may remain. Reaching beyond the surficial portion of the heap may require the direct application of leachate through drilling and injection (Seal, 2004, 2007). Leachate injections can be gravity fed or under pressure, and methods have been developed to systematically re-stimulate the entire length of the well column (e.g., Newmont's patent pending Hydro-Jex process).

Rucker (accepted for publication) and Rucker et al. (2009) discussed methods of siting secondary recovery wells within a heap to maximize the potential of extracting the highest grade ore. Three-dimensional electrical resistivity was used to map the high and low resistivity targets within a heap and it was found that generally low electrical resistivity is associated with higher moisture and lower gold content. The low resistivity regions could be the result of fine-grained materials retaining moisture or preferential flow paths that have established in the heaps. In a few cases, the opposite was shown to occur, where low resistivity was associated with higher gold content. The gold could have been initially associated with fines or is tied up in easily extracted (water leachable) pockets of perched leachate. The study by Rucker (accepted for publication) also showed that the heaps were electrically heterogeneous with high and low resistivity material within a few tens of meters from each other.

Once a well has been sited and restimulation through injection started, there are no assurances that the leachate will flow evenly across the stimulation zone. Through active monitoring of the

* Corresponding author. Tel.: +1 520 647 3315.

E-mail addresses: druck8240@gmail.com (D.F. Rucker), mmcneill@hgiworld.com (M. McNeill), Al.Schindler@Newmont.com (A. Schindler), gnoonan@hgiworld.com (G. Noonan).

¹ Tel.: +1 520 647 3315.

injections, one can verify leachate coverage. The information gained through monitoring is also necessary to effectively decide which is the next stimulation well as operators move through the succession of wells. The same low permeability zones that disrupt flow during surface leaching can impact flow and drainage during the injection. Monitoring would show in which direction the leachate is tending to flow, and the operators would likely move towards the drier directions.

Options for monitoring are hydrologic-based sensors buried in heaps, such as tensiometers (Menacho et al., 2007) or time domain reflectometers (Walker and Powell, 2001). These point-based measurements would have to be nested to cover multiple depths and staged sufficiently around the injection point to ensure complete capture. As in characterization, electrical resistivity offers a practical volumetric imaging technique. Although multiple parameters can influence the final measured resistivity values (e.g., water content, clay content, porosity, pore water constituents), the change in resistivity over time will necessarily be reflective of the changes in pore space saturation.

This work demonstrates the concept of continuous electrical monitoring of a secondary recovery process by presenting resistivity data during a high pressure injection of leachate into a gold heap at Newmont's Twin Creeks mine. Other works in the area of electrical monitoring of fluid movement in unsaturated systems have been presented (Daily et al., 1992; Cassiani et al., 2006; Batlle-Aguilar et al., 2009). Our approach diverges significantly from these past works by presenting results of both two- and three-dimensional analyses over multiple injections at different depths within an active heap. Two injections are shown, with each injection occurring over a three-day span. To help place the results in perspective, hypothetical examples

are also given to show how the measurement system should respond to simple shaped leachate plumes.

2. Site description

The Twin Creeks mine is located approximately 35 miles north of the town of Golconda, Nevada (Fig. 1). The mine consists of a single large active open pit mine, overburden piles, topsoil stockpiles, tailings impoundments, and heap leach facilities. Mining originally began in 1986 in the northern part of the project area as the Chimney Creek mine. In 1989, the Rabbit Creek mine in the southern portion of the project area began mining. In 1993 Chimney Creek and Rabbit Creek mines were combined and renamed Twin Creeks to pursue development of a large sulfide deposit. Newmont Mining Corporation merged with the owner of the Twin Creeks operation and became Project Owner and Operator in 1997.

The Twin Creeks mine is hosted in decalcified, silty limestone of the Ordovician Comus Formation, sheared and decalcified dolomitic siltstone of the lower Valmy Formation, faulted and sheared argillized pillow basalts of the upper Valmy Formation, and decalcified, silty limestone of the Etchart Formation (Schutz et al., 2004). More detailed descriptions of the geology and mineralogy of the mine can be found in Simon et al. (1999), Hall et al. (2000), and Fortuna et al. (2003).

The heap under investigation for this injection and monitoring study was the southern Osgood heap. Fig. 2 shows the heap with the layout of injection wells. The Osgood heap was constructed using a 60 mil HDPE synthetic liner over a compacted soil base. A series of PVC pipes collect the pregnant solution, which is then directed to synthetically lined process ponds. The ore was placed on the heap in a series of lifts that range from 10 to 17 m in height.

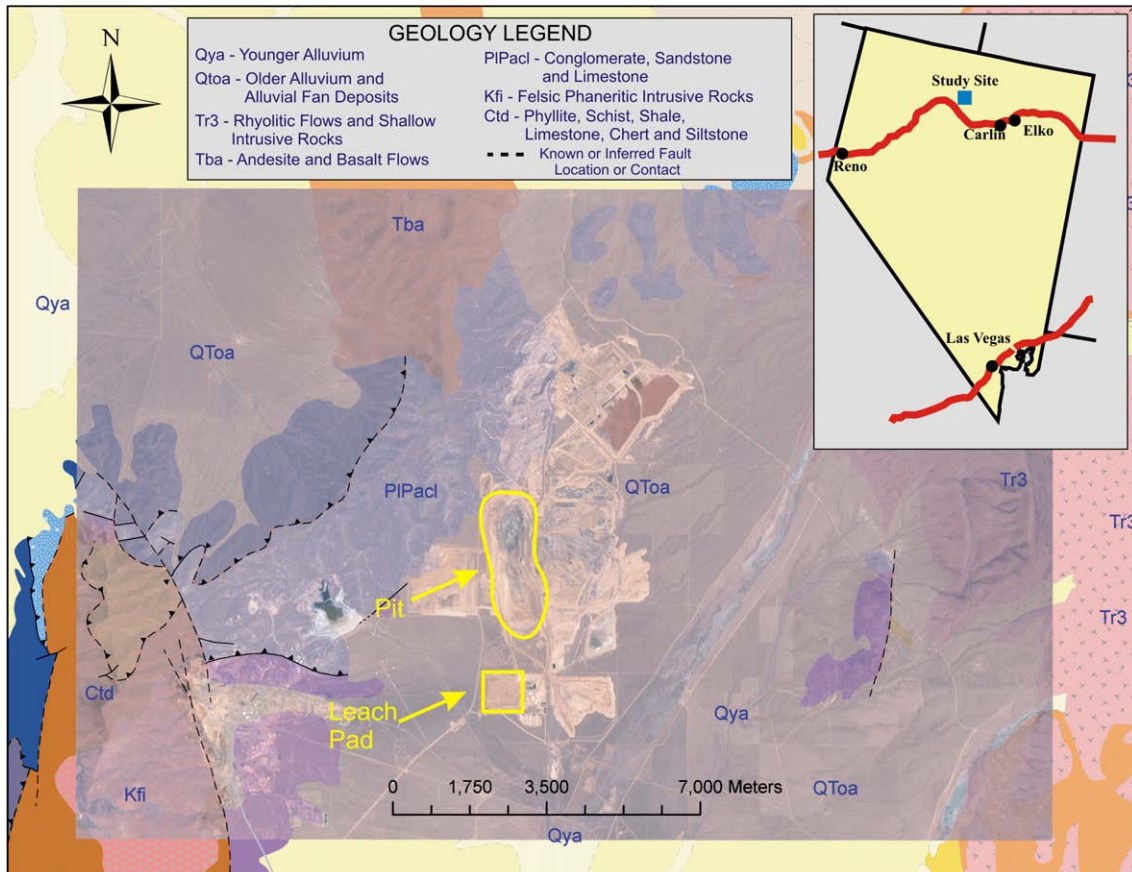


Fig. 1. Site location of the Twin Creeks mine with geology (geologic data adapted from Crafford, 2007).

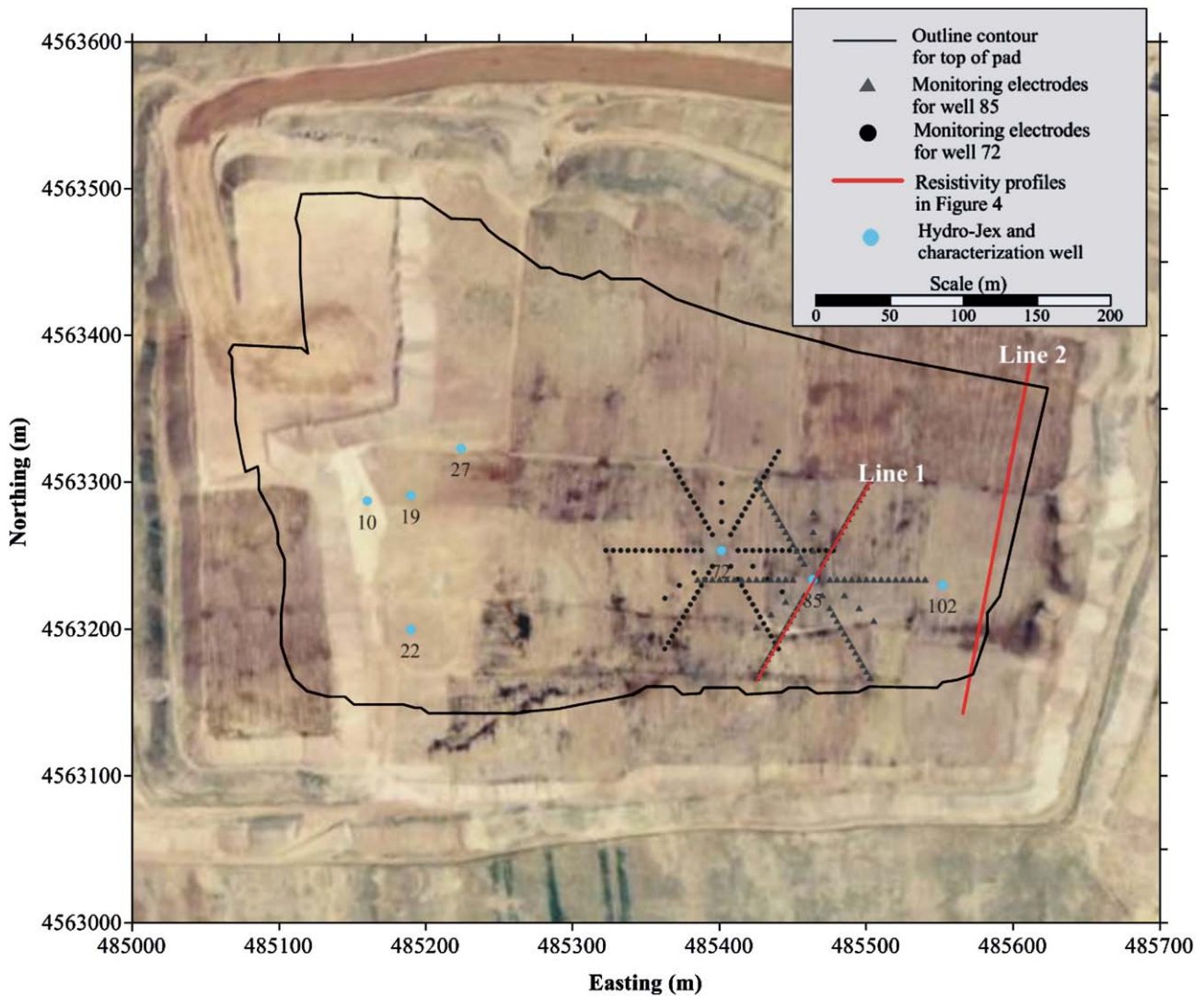


Fig. 2. The Osgood heap with Hydro-Jex wells, characterization wells, and resistivity survey line layout.

Assay results of several wells across the heap, showing gravimetric moisture (as a percentage) and leachable gold (aurocyanide in ounces per ton), are presented in Fig. 3. Rock samples were collected every 1.5 m from the surface to 57 m below pad surface. Wells 10 and 19 (Fig. 3A and B) in the west generally show higher gold concentrations as calculated from the arithmetic average across the depth. Additionally, Fig. 3E and f show a strong negative correlation of gold with moisture for these two wells, with a correlation coefficient of -0.45 and -0.49 for well 10 and 19, respectively. Well 85 (Fig. 3C) appears to have the highest average moisture content at 7.2% and is approximately 30% higher than the other three wells. In the depths from about 20 to 50 m, the average increases to 8.2%. The correlation of moisture with gold is weakly positive for this well (Fig. 3F), possibly indicating that the gold is found mainly in the fines or the gold is already leached and ready to be released through simple rinsing. Well 102 in Fig. 3D and h shows an overall low gold content and low moisture with no correlation between the two variables.

Two electrical resistivity profiles are presented for the Osgood heap in Fig. 4; one at the injection of well 85 (the northeast-southwest radial leg – referred to as Line 1) and the other on the eastern flank of the heap (Line 2) near well 102. Rucker et al. (2009) describes the methodology of acquisition and processing for the resistivity data. The profile at well 85 was acquired prior to the injection using a pole-pole array and the eastern Line 2 was acquired during the course of the

second day's injection with the gradient array. When Line 2 was acquired, the solution had not reached the line's location as verified by a follow-up measurement on the line two days later. It is believed that the electrical resistivity distribution of Line 2 is representative of pre-injection conditions.

The resistivity data show a similar trend as the moisture, that is, the resistivity is higher towards the east in Line 2. There are a few pockets of lower resistivity material within Line 2, which could be isolated zones of fines retaining moisture. Line 1, on the other hand, shows an entire thick layer of lower resistivity material from 20 to 40 m below pad surface. In addition, there appears to be a very low resistivity plug at the location of well 85, with resistivity values as low as $4 \Omega \text{ m}$. The plug extends below a depth of 50 m and the resistivity data appear to correlate strongly with moisture in the well. There is also a higher resistivity layer above the low resistivity layer and this stratification may be associated with the different lifts. Line 2 also shows some signs of weak stratification and several features to the north and south could be thought to have been connected at one point.

3. Hydro-Jex injection

Seal (2007) describes the Hydro-Jex process as a three step procedure of 1) drilling and characterization, 2) stimulation with high pressure pumping to create new solution paths while adding reagent

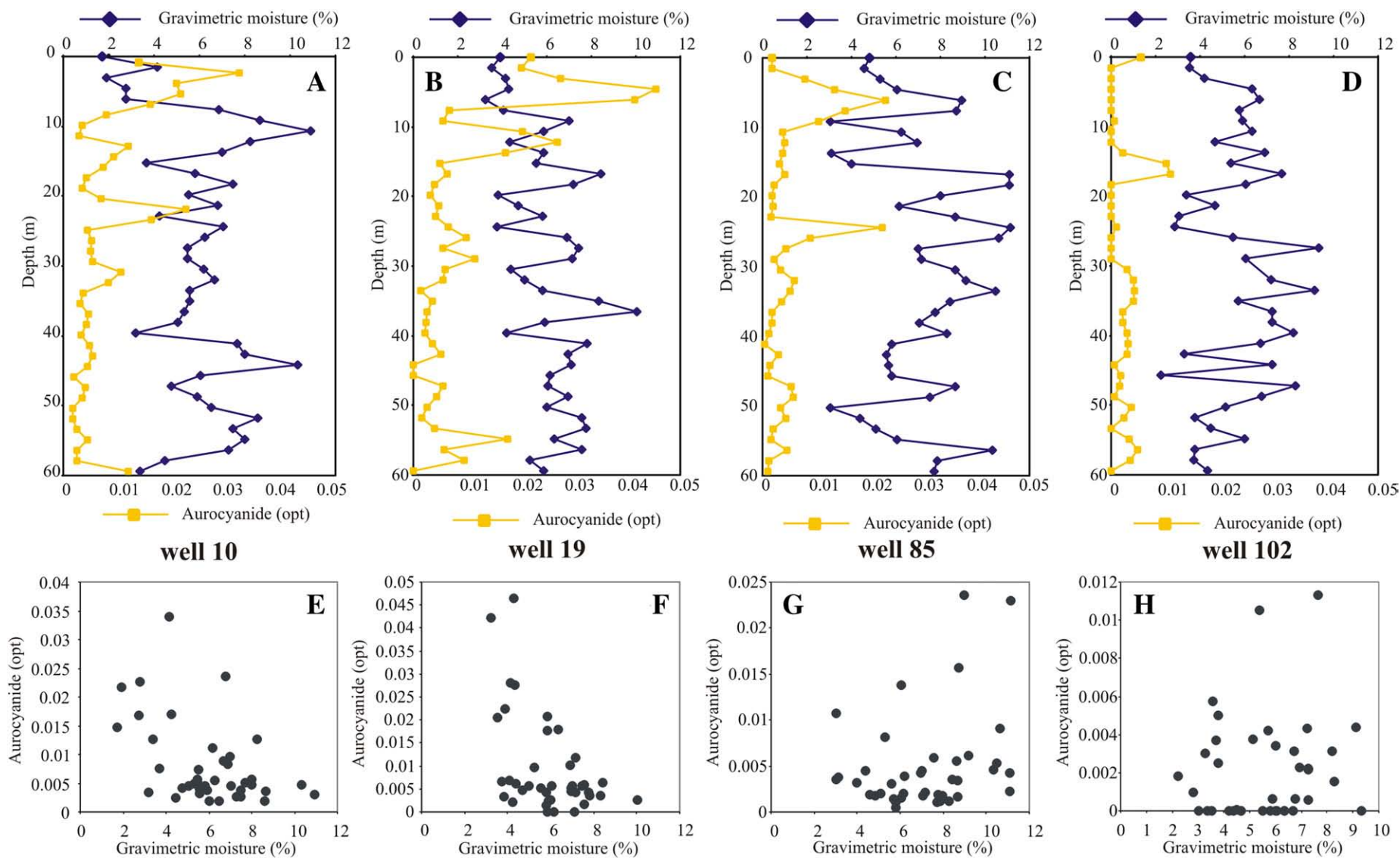


Fig. 3. Moisture and leachable gold content from wells within the Osgood heap, presented as depth profiles in A-D and scatter of moisture versus gold for E-H.

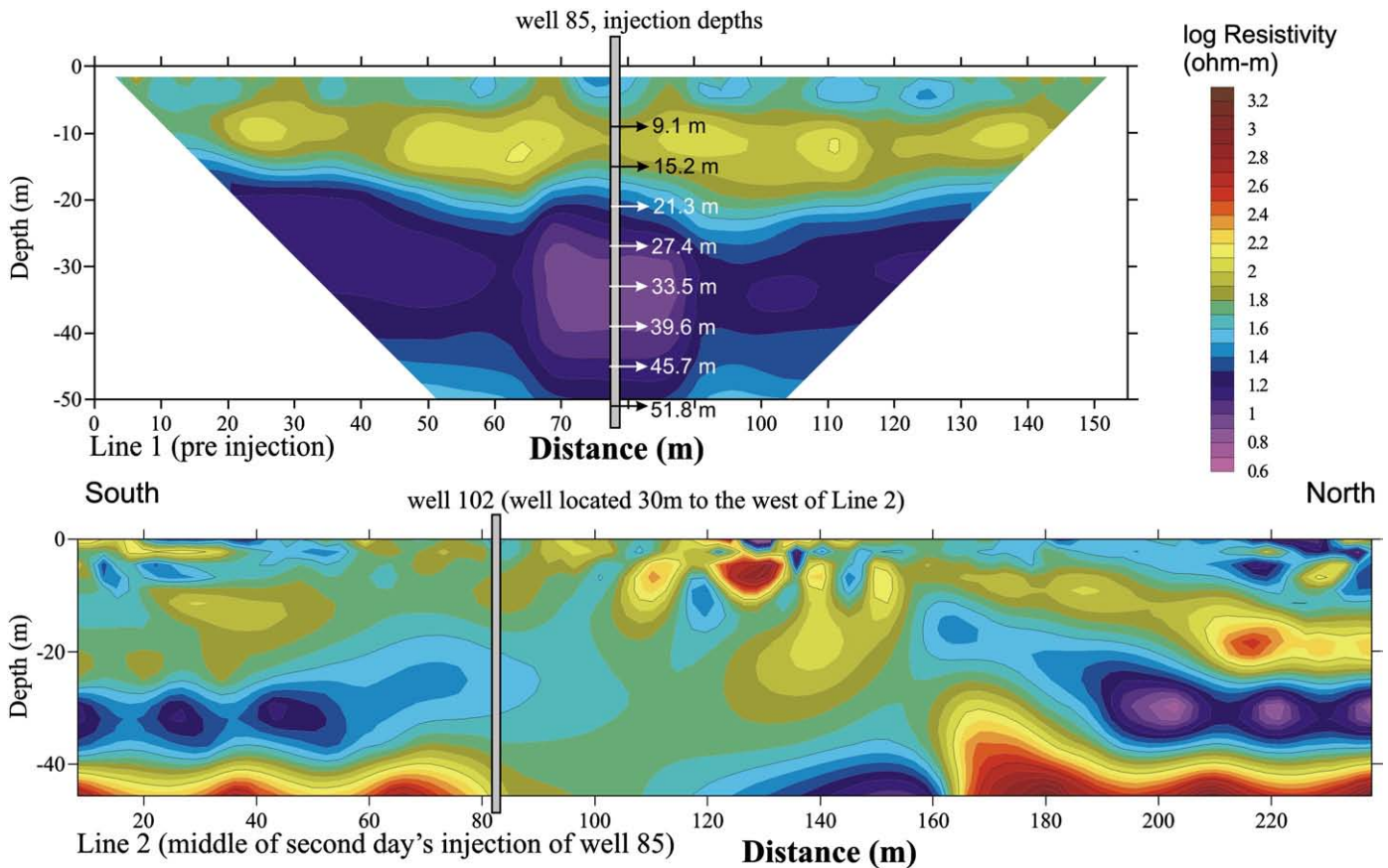


Fig. 4. Pre-injection resistivity characterization of two lines across the Osgood heap. Line locations are shown in Fig. 2. Line 1 is centered on well 85 and line 2 is along the eastern edge the heap.

to targeted zones of under-leached ore and 3) gravity rinsing with solution to further enhance metal recovery. The duration of each step depends on the targeted depth, but generally requires 1–2 days for drilling, 2–4 days for stimulation, and up to 10 days for rinsing. In step one, the drilling is conducted by advancing the casing simultaneously. The casing is then perforated after installation to target specific zones. The characterization can be a combination of assaying and electrical resistivity. Rucker (accepted for publication) showed how assaying alone may not be adequate for describing the spatial distribution of hydrological and metallurgical parameters. The characteristic length scale describing the similarity of nearby assay values in adjacent wells is likely larger than the average separation between wells. This fact makes interpolation with assay data alone tenuous, and resistivity offers a means to bridge the gap.

For step two, the high pressure stimulation process typically occurs at multiple zones within the lift, say every 6.1 m. Packers are used to isolate these zones. Each zone is injected separately for about 2 h at a rate of about 3000 L/h. For the Twin Creeks injections, the first injection started around a depth of 51.8 m for well 85 and 57.9 m for well 72. The last injection for both wells was at a depth of 9.1 m. The injection pressures are high enough to theoretically open up channels by hydrofracturing the heap, i.e., injection pressures are greater than the lithostatic pressure of the overburden. For the Twin Creeks injections, pressures were generally between 750 and 1200 kPa, depending on depth. Fig. 5A and B shows the injection schedule for wells 85 and 72. The time series of injection pressures for each well (Fig. 5A) and cumulative injection volume (Fig. 5B) for each zone is presented. Approximately 350 m³ of reagent is injected in each zone.

In the third rinsing step, each zone is re-leached with a gravity feed. Permitting issues prevent the rinsing step to be combined with

active injections in the same heap, so the process of injecting and rinsing occurs serially from one well to the next. When the initial rinsing of the last well is completed, the solution is moved to the first well again and the re-rinsing is cycled through each zone of every well. The initial rinse allows for the slower rate kinetics to diffuse residual metal from micropores, vugs, and fractures, until solution is reintroduced on the second rinse. The rinsing typically occurs at less than 1900 L/min, again due to permitting requirements.

The success of the Hydro-Jex process was demonstrated at the Lone Tree mine (Seal, 2007). Four wells were drilled into the pad and the pregnant leach solution from the stimulated Hydro-Jex field was collected in isolated ponds. The resulting metal values showed variability of 20–80 troy gold ounces per day. These values equate to a resultant 12.7 troy gold ounces/meter drilled over a six week period. An additional benefit was the increased pH of the heap through reagents added during stimulation.

4. Overview of electrical resistivity monitoring

Electrical resistivity is a function of the heap's moisture content, porosity, degree of fines, concentration of lixiviant, temperature, and other factors that can add together constructively or destructively to form the final resistivity value. Mapping the resistivity from the surface, as shown by Rucker et al. (2009), requires a calibration from assay data to fully understand the spatial distribution of the parameter of interest. Large targets of contrasting resistivity values (e.g., high and low resistivity), however, may be generalized, as there are usually only a couple of parameters in a heap that tend to drive the system, including moisture and clay content. The resistivity calibration with additional assay data can hone the regression models used to convert from resistivity to the desired heap property.

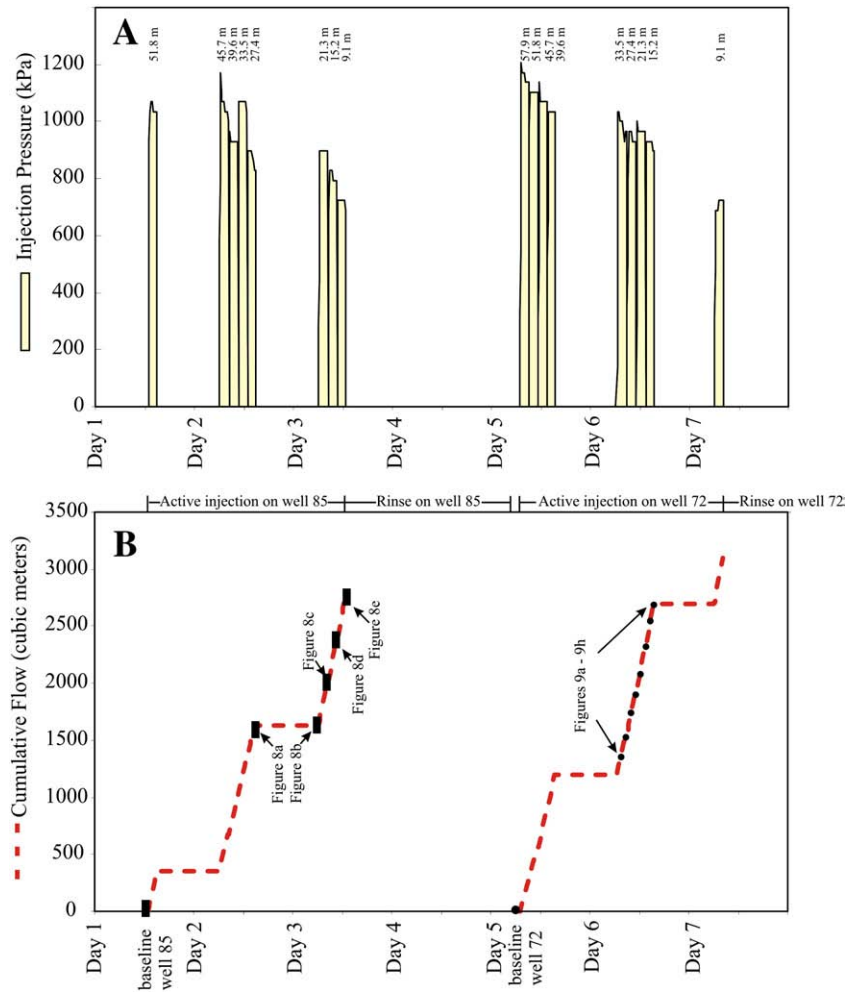


Fig. 5. Injection parameters for the Hydro-Jex secondary recovery method applied to wells 85 and 72. A) Injection pressures for each zone, with depth of injection indicated over each bar and B) Cumulative volume. Boxes along the cumulative flow curve in well 85 indicate snapshots of resistivity images in Fig. 8. Circles along the cumulative flow curve for well 72 indicate snapshots of resistivity images for well 72.

The changes in electrical resistivity over time may be uniquely related to changes in moisture content of the heap by considering that all other parameters are static. The static assumption is particularly valid if the measurements are conducted over short time periods. Temperature, especially, may have a significant role in changing the resistivity values of the near surface if measurements are conducted over long time periods (Hayley et al., 2007). For short time periods, an injection of a fluid of constant ionic strength will change only the liquid saturation of the pore space and monitoring the changes in resistivity can give some indication of these changes. Daily et al. (1992) first demonstrated the concept by electrical monitoring of a 1900 L injection of tap water at the surface into an undersaturated soil. The resistivity data were consistent with other supporting measurements and knowledge of the site.

The relationship between saturation and resistivity is exponential, as described by Archie's equation (Archie 1942; Schon, 1996):

$$\rho_t = a\rho_w\phi^{-m}S_w^{-n} \quad (1)$$

where ρ_t is the resistivity of the rock with fractional saturation, n is the saturation index, ϕ is the porosity, a and m are empirical fitting parameters to complete the description of the rock resistivity, and ρ_w is the resistivity of the water. Keller (1988) suggests $n = 2$ for sand and many have used this value for their work (see Edwards, 1997; Descloitres et al., 2008), while others have observed values less than

$n = 2$ (Taylor and Barker, 2002). Grellier et al. (2008) used $n = 2.5$ for a landfill application, and Sen (1997) discussed some reasons for n deviating from its "normal" value of $n = 2$. Regardless, if $m = n$, then Eq. (1) can be reduced to

$$\rho_t = a\rho_w\theta_v^{-n} \quad (2)$$

or

$$\rho_t = a\rho_w(D_b\theta_g)^{-n} \quad (3)$$

where the substitution of $\phi^{-n}S_w^{-n}$ is made for the volumetric water content (θ_v). In Eq. (3), another substitution of gravimetric water content is made for volumetric water content, by incorporating the bulk density (D_b) in g/m^3 . Guzman et al. (2008) described several relationships of dry bulk density as a function of heap height, where the bulk density was observed to increase up to 30% at 80 m BPS.

The time derivative of Eq. (1) would remove the dependency of non-saturation related parameters and one could set up a system on nonlinear equations to solve for both n and S_w at any point in time if the equation set is constrained by at least one known value of S_w . Additionally, the set of equations would have to be created at every point in space. The S_w information is never known except for numerical flow models and the alternative to the problem is to

simply present the percent change of resistivity (%ρ) from a baseline condition:

$$\% \rho^1(x, y, z) = \frac{\rho_t^1(x, y, z) - \rho_t^0(x, y, z)}{\rho_t^0(x, y, z)} \cdot 100 \quad (4)$$

where the superscripts indicate a snapshot in time, and superscript 0 representing the baseline. Calculations conducted in this way allow relative changes to be compared equally. A 20% decrease from 100 to 80 Ω m or 10 to 8 Ω m are represented by the same isopleth.

5. Hypothetical modeling

As an example of electrical monitoring of an injection, consider the following parameters: a radial arrangement of electrodes on the surface of the heap, exactly like that shown in Fig. 2, are separated by a nominal 5 m along each radial arm. The length from one end of a radial arm to the other is 155 m. The radial arrangement of electrodes from a central injection is preferred to other electrode arrangements due to wiring; multi-conductor cables allow the efficient use of wire along linear segments of the array. The alternative, an even distribution of electrodes over the area, requires individual wires to be run from the electrode to the resistivity meter. For the same area as the radial arrangement, electrodes would be spaced 17 m apart for an even distribution, and the ground wires would be in the way of the drilling and injection equipment.

A pole–pole electrode array is also used, where the typical four-pole electrode setup of two electrical current transmission and two potential (voltage) receiver electrodes are modified to place one pole from each pair effectively far from the survey area. Each electrode internal to the measurement array will have a turn at passing current while all others will measure the voltage. For a 94-electrode system, a total of 4371 measurements (of non-repeat pairs) will be acquired.

For simplicity, the hypothetical heap is represented by a homogeneous 100 Ω m background. A 355 m³ injection occurs at multiple depths and the leachate occupies on average an additional 3.7% of the matrix volume, equivalent to changing the volumetric water content from 0.15 to 0.187 m³/m³. The leachate plume has a constant thickness of 4 m at each depth and the final simplified square plume is 48.6 m on a side. The plume is represented by a constant value of 10 Ω m and the resistivity array at the surface is used to conduct the electrical measurements. For each injection depth it is assumed that the plume fully drains from the heap before the next injection occurs. The resulting dataset from the hypothetical model includes the voltage normalized to current (i.e., transfer resistance according to Ohm’s Law), and would be the same dataset as if the system were set up over a real heap. This hypothetically measured dataset is then inverse modeled with the finite difference method to back-calculate the resistivity distribution of the heap that gave rise to the voltage measurements. The inverse modeled plume will not represent the starting conditions with absolute fidelity. Differences can be attributed to loss of sensitivity of the measurement system for deep plumes and too few measurements relative to the number of finite difference cells, requiring additional constraints to formulate a unique answer. The typical constraints are to limit the final values of calculated resistivity to be within a particular range and smoothing (small values in the spatial derivative of resistivity).

Fig. 6 shows the results of modeling the 10 Ω m plume in a 100 Ω m background. The RES3DINV resistivity inversion code was used to model all data in three dimensions. The results are presented as contours of percent change according to Eq. (4), with sub-plots A and C representing an injection at 57.9 m and sub-plots B and D representing an injection at 9.1 m. Both overhead (horizontal slices) and side (profiles through the center of the volume) views are shown. The different injection depths are presented with separate contouring based on the sensitivity of deep plumes versus shallow plumes. What is shown here is that the shallow plume is represented more accurately than the deep

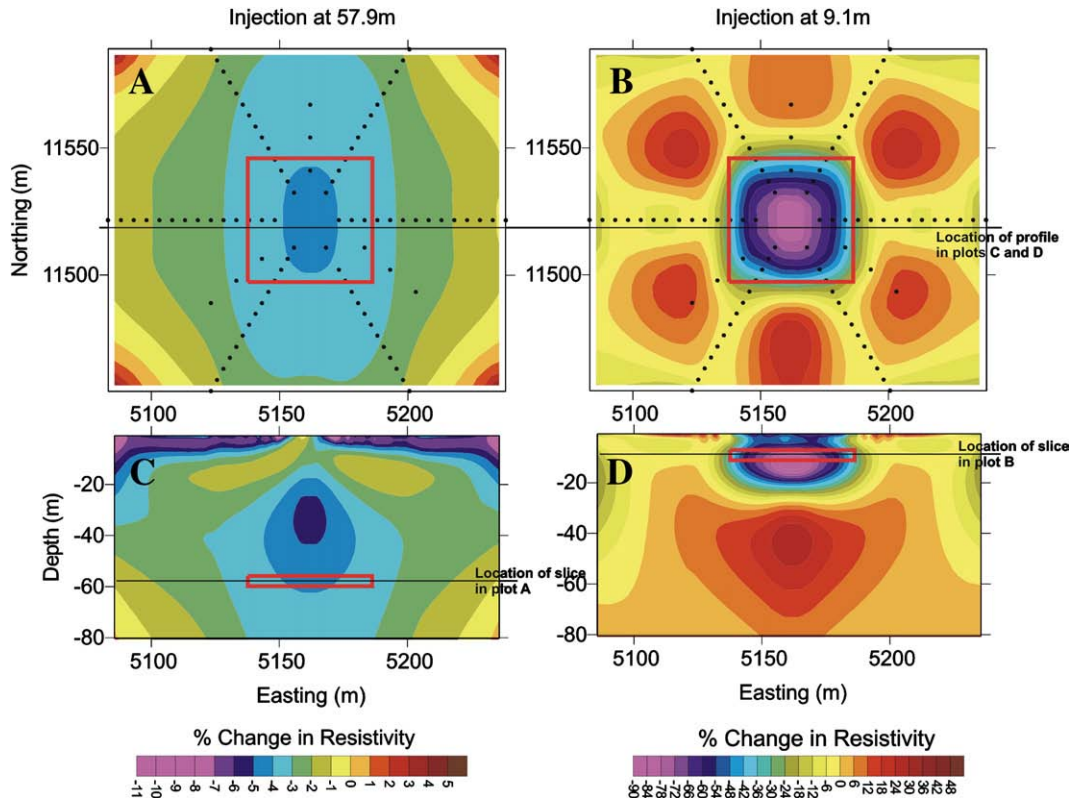


Fig. 6. Resistivity modeling of a hypothetical plume at a depth of 57.9 m and 9.1 m, demonstrating the differences in sensitivity for the different zones.

plume. The horizontal slice of Fig. 6B shows that the percent change in resistivity can match the distribution quite well. In addition, the profile in Fig. 6D poses the reconstructed plume at the depth of the injection. However, there is some vertical smearing of information due to the smoothing constraints employed in the inversion procedure. Additionally, some regions show an increase in resistivity relative to background implying a decrease in saturation. These are artifacts due to the fitting procedure of the inversion methodology.

The inversion results for the deep moisture plume in Fig. 6B and D under-represents the actual plume by placing the plume's center approximately 20 m above its real location. Additionally, the plan view shows that it is highly smeared in the north–south direction. The smearing and inaccurate depth location is again due to the lack of sensitivity of the method away from the electrodes (Singha and Moysey, 2006). Resolution of deep moisture plumes can be enhanced by directly placing electrodes deeply within the heap or by imaging taller plumes. Based on the hypothetical modeling, only those injections from the field measured data more shallow than 33 m will be presented.

6. Geophysical survey method

Throughout the seven day injection period on wells 72 and 85, resistivity data were acquired at the surface of the heap using a radial array of electrodes (Fig. 2) spaced 5 m apart. Each injection well had its own set up, with the radial arms emanating from the well. A 94-channel GEO-Scope resistivity meter (hydroGEOPHYSICS, Inc, Tucson, AZ) was used to acquire the data using a pole-pole array. The two infinite poles for the array were placed far from the survey area, but still within the confines of the heap.

Cycling through each of the 94 transmitter electrodes would have required 24 min to complete, given the number of repeat measurements, current on-time, auto-gaining of signal, and other internal hardware and firmware steps. Within this time frame, the moisture plume would have changed significantly and the first and last measurement likely would not have represented the same state of the plume. Therefore, the electrodes were divided into thirds evenly throughout the array and the sequencing of measurements occurred by acquiring data for the each of the thirds. A partial dataset would be acquired in this manner every 8 min, and it would be enough to invert for plume shape and extent. The active injection period of 48 h on wells 85 and 72 produced almost 350 data files for each injection.

Fig. 7 shows an example time series of transfer resistance for the injection well 72. The transmitter–receiver pair is electrode numbers 92 and 34, which is in the center of the northeast and northwest leg

respectively. The times of injection and injection depth are also presented to demonstrate the effects of the various injections on the resistance measurements. The time series of resistance shows an increase in resistance during inactive times and decrease in resistance during active injections. Before injection occurs on Day 5, for example, the resistance is increasing as the leachate drains from the heap after the cessation of injection on well 85. As soon as the injections start on well 72, the resistance drops. Interestingly, the measurement system has sufficient temporal resolution to distinguish when the packers are deflated to move up to the next injection. The momentary pause and subsequent drop in time series character aligns quite well with the timing of the injections. Then, at the end of the day's injection, the resistance begins its recovery. The shape of these injections and recoveries are similar to that of monitoring drawdown and subsequent recovery during the pumping of a confined aquifer.

The signal noise was evaluated by fitting a polynomial curve to the inactive portion of the time series from the end of the injection on Day 5 to the beginning of the injection on Day 6. The residual, or difference between the fit and measurement was found to be 0–3% of the difference between the maximum and minimum value of the entire time series record.

7. Geophysical results

At any point in time, the data from all available combinations are extracted from the time series and inverse modeled. In Fig. 8, a series of inversion models are shown from well 85, where the data from the northeast–southwest alignment (Line 1 in Fig. 2) were inverse modeled in two-dimensions using Earthimager2D (Advanced Geosciences, Inc. Austin, TX). The inverse modeling results are shown as profiles and the well is located at the center ($x=77.5$ m). The snapshots from each inversion are compared to the baseline acquired prior to any injection occurring, and the plots in Fig. 8 show the percent change from this baseline according to Eq. (4). Fig. 5 shows graphically the times of each snapshot.

Fig. 8A shows the distribution of resistivity change at the end of the 2-hour injection at a depth of 27.4 m, which also corresponds to the last injection of day 2. The figure represents the changes in resistivity due to the combined injections from 51.8 m to 27.4 m. Using the intensity of the resistivity change as a direct indicator of changing saturation, the data appear to show a preferential flow of the moisture plume towards the northeast. The increasing saturation is elongated laterally out to 95 m then has a strong vertical component, likely drainage of the pregnant leach solution out of the pile. Fig. 4 shows a

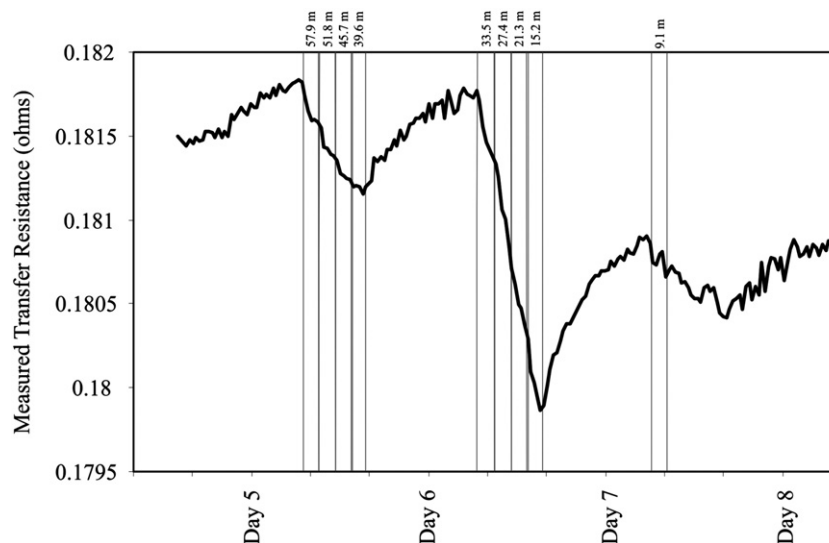


Fig. 7. Example transfer resistance time series record for well 72.

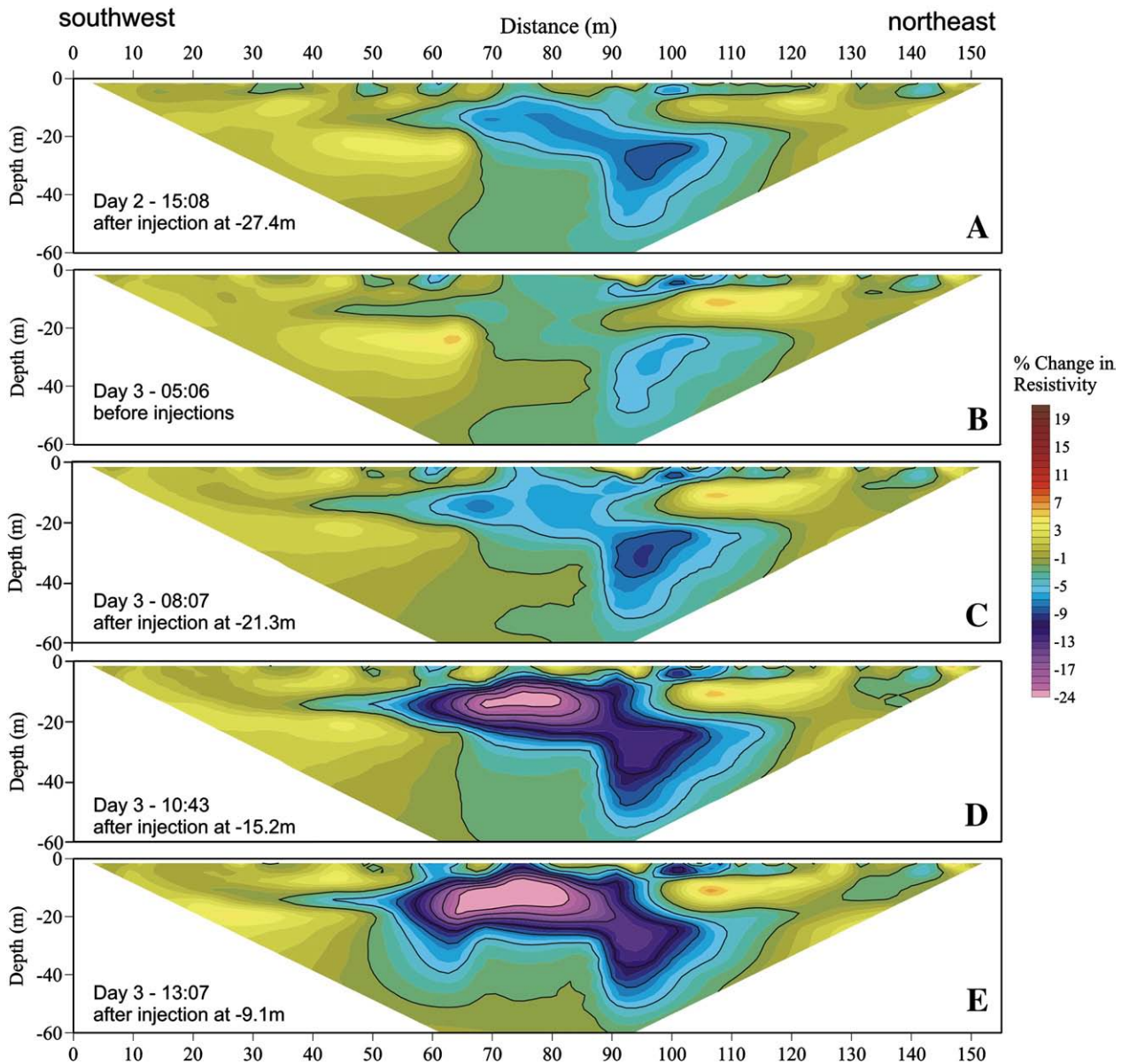


Fig. 8. Snapshots of resistivity profiles during injections on well 85. Times of the snapshots are indicated within each sub plot, and are also shown graphically in Fig. 5B.

low resistivity plug out to this distance and the flow around the plug could be due to a low permeability region of fine grained material.

Fig. 8B through e show the results of the third day's injection. Fig. 8B shows the distribution prior to beginning any work, and the intensity of the change in resistivity is less than that of Fig. 8A. Much of the leachate likely drained from the heap by this point, but the profile does show a thin layer of lower resistivity heading towards the southwest. This could indicate a channeling effect though coarser grained material. After the injection at 21.3 m (Fig. 8C), the channeling is more prevalent, but so too is the drainage along the northeastern corner of the plug. Based on the changing sensitivity of this resistivity method to depth, it is best to compare shapes of the contours from one injection to another and not contour value (other than Fig. 8A and B, which can be compared). With this in mind, the injection at 15.2 m (Fig. 8D) does not appear to be extending the leachate out to more regions in the direction of the profile. However, the injection at 9.1 m (Fig. 8E) indicates that new drainage pathways are occurring at the southwest corner of the low resistivity plug. All together, the high pressure injections appear to be pushing liquid out laterally to at least 25 m from the source, with a few channels opening up to about 40 m from the source.

Fig. 9 shows the time-lapsed resistivity results from the injections on well 72. Again, the sections were created by comparing the data to the baseline condition at a time before injections started on well 72. To create these images, the resistivity data were inverted in three dimensions using RES3DINV. Horizontal slices were extracted from the volume of resistivity data and contoured for each snapshot in time. The eight sub-plots are taken from the depth of the injection volume for Day 6 only, where injections occurred at depths of 33.5, 27.4, 21.3, and 15.2 m. Also, for each injection, two images are shown that represent the middle and the end of each two hour injection period.

The images show a progression of decreasing resistivity from the center injection well. There also appears to be a potential artifact in all of the images along the western edge of the model domain and further discussions of leachate movement will ignore this feature. At a depth of 33 m, the fluid appears to be migrating preferentially to the east. Using the -4% change as a guide, the area of influence at the 33 m depth increases from 454 m^2 to 1805 m^2 , with a distance of 60 m from north to south for the later time period. If the leachate plume is fairly horizontal, no significant drainage has occurred, and the plume height

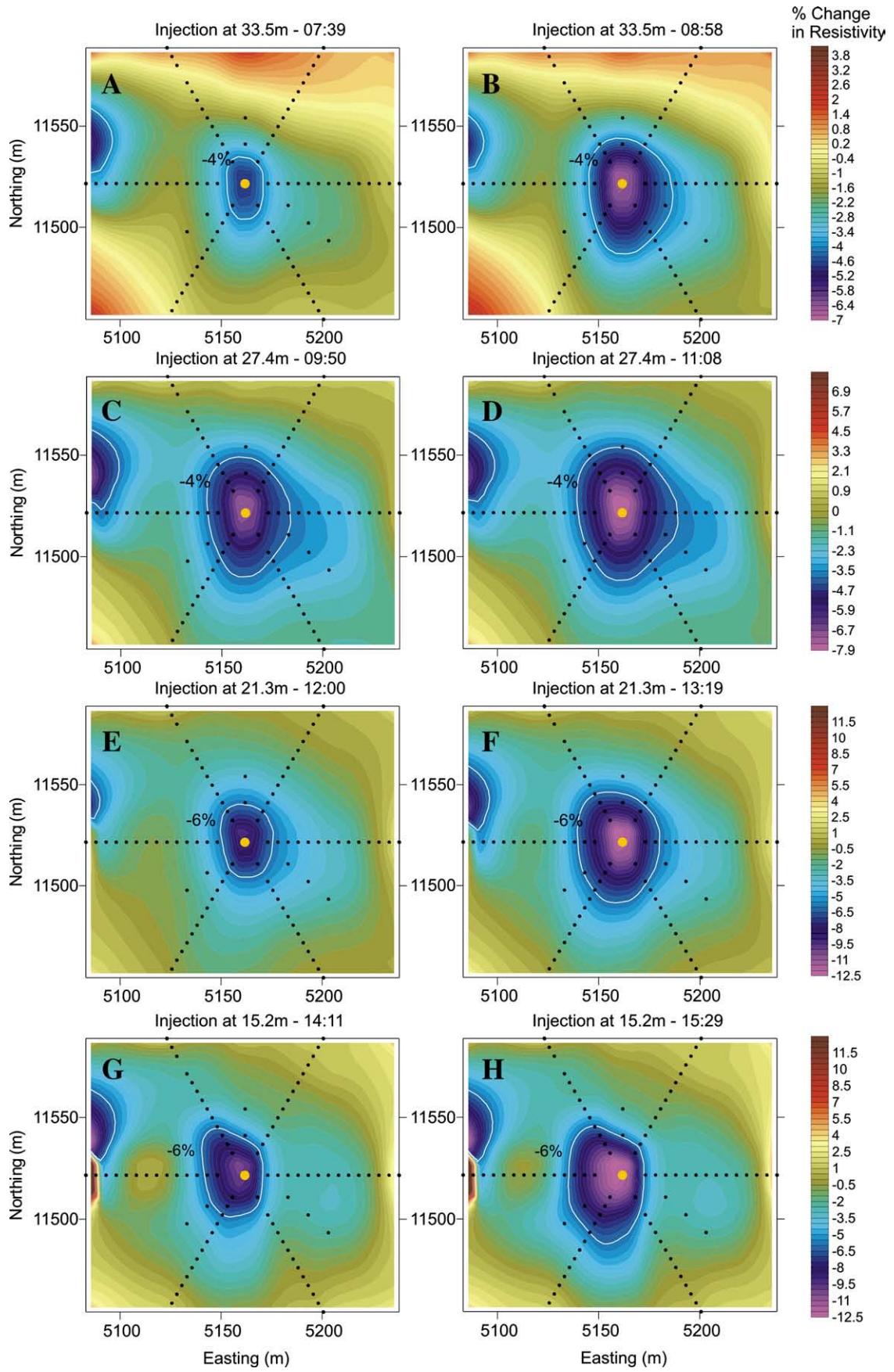


Fig. 9. Snapshots of resistivity slices during the injections on well 72. The horizontal slices are at the depths of injection. Times of the snapshots are indicated within each sub plot, and are also shown graphically in Fig. 5B.

is an average of 4 m, then the water content changes by an average of 20% for the early time and 5% for the later time. Regions outside the –4% contour would see an even smaller increase in water content. Even at these high volume flow rates, the heap likely does not become fully saturated within the injection zone far from the wellbore.

Progressing through the injection depths and times, the shape of the moisture plume for the selected isopleths are fairly consistent with minor variability from zone to zone. There is slight anisotropy as the plume will tend to move towards one direction. For example, the 15.2 m depth shows the plume moving initially northwest, then south. It is difficult to understand the exact level of moisture content changes, however, directly from the resistivity. It is recommended that an increase in utility of resistivity to monitor these events can be made if a few moisture sensors were buried in the specific zones of injection. Additionally, deeply buried and nested electrodes would help increase the sensitivity of the method deeper in the heap and allow a direct comparison from one zone to another.

8. Conclusions

A secondary recovery application was monitored using electrical resistivity geophysics to more fully understand the effectiveness of leachate movement and the recovery methodology. The secondary recovery method involved high pressure injections of leachate deeply into a heap. Two injection wells were monitored for seven days, where approximately 3000 m³ of fluid was added in each well at multiple zones. The major findings of the work are:

- The electrical resistivity method as applied from the surface could sense changes in resistivity, likely resulting from changes in saturation or moisture content of the void space. Decreases in resistivity can be related to increasing moisture from the leachate injections.
- Due to the sensitivity of the method for injections over thin horizons, the inverse modeling does not properly represent the depth of the plume for plumes below 33 m.
- Adding deep electrodes into the heap or monitoring thicker injection zones would increase the sensitivity of the method.
- The injections exhibited interesting behavior for well 85, where a low permeability plug prevented leachate from draining through it. The resistivity data indicated that the leachate moved along the top of the plug until it reached the edge before cascading over the edge.
- Based on the injection pressures, the Hydro-Jex method is likely hydrofracturing the heap to open up thin horizons along bedding planes. The resistivity data indicates that the horizons may extend an extra 20 m beyond the main body of the moisture plume.
- By picking a constant isopleth for a particular injection zone, rough estimates of hydrologic parameters can be estimated. For this example, we used a 4% decrease in resistivity to understand the changes in moisture content through time. At early times within each zone, the resistivity shows that the heap is potentially saturated near the wellbore. At later times, the size of the isopleth indicates a smaller average change in moisture content. Hydrologically, this is well founded as the pore pressures decrease away from the injection zone.
- There appears to be some anisotropy in the hydraulic properties of the heap to cause the plume to migrate in particular directions. Based on the injections on well 72, it would have been advised to move north and west as the heap appears less affected and drier in that direction.
- Calibration of the resistivity method could be conducted if a few moisture sensors were part of the monitoring processes.
- As a final recommendation to heap operators, the resistivity electrodes could be installed as the heap is being built. The optimum design would place electrodes on the bottom of the heap and between each lift. With this design, the heap could be monitored during both primary and secondary recovery steps.

References

- Archie, G.E., 1942. The electrical resistivity log as an aid in determining some reservoir characteristics. *Transactions of the American Institute of Mining, Metallurgical, and Petroleum Engineers* 146, 54–62.
- Battle-Aguilar, J., Schneider, S., Pessel, M., Tucholka, P., Coquet, Y., Vachier, P., 2009. Axisymmetrical infiltration in soil imaged by noninvasive electrical resistivity tomography. *Soil Science Society of America Journal* 73, 510–520.
- Cassiani, G., Bruno, V., Villa, A., Fusi, N., Binley, A.M., 2006. A saline trace test monitored via time-lapse surface electrical resistivity tomography. *Journal of Applied Geophysics* 59, 244–259.
- Crafford, A.E.J., 2007. *Geologic Map of Nevada: U.S. Geological Survey Data Series 249, 1 CD-ROM*, 46 p., 1 plate.
- Daily, W., Ramirez, A., Labrecque, D., Nitao, J., 1992. Electrical resistivity tomography of vadose zone water movement. *Water Resources Research* 28, 1429–1442.
- Decker, D.L., Tyler, S.W., 1999. Evaluation of flow and solute transport parameters for heap-leach recovery materials. *Mining Engineering* 28, 543–555.
- Desclotres, M., Ribolzi, O., Troquer, Y.L., Thiébaux, J.P., 2008. Study of water tension differences in heterogeneous sandy soils using surface ERT. *Journal of Applied Geophysics* 64, 83–98.
- Edwards, R.N., 1997. On the resource evaluation of marine gas hydrate deposits using sea-floor transient electric dipole–dipole methods. *Geophysics* 62, 63–74.
- Fortuna, J., Kesler, S.E., Stenger, D.P., 2003. Source of iron for sulfidation and gold deposition, Twin Creeks Carlin-type deposit, Nevada. *Economic Geology* 98, 1213–1224.
- Grellier, S., Guérin, R., Robain, H., Bobachev, A., Vermeersch, F., Tabbagh, A., 2008. Monitoring of leachate recirculation in a bioreactor landfill by 2-D electrical resistivity imaging. *Journal of Environmental and Engineering Geophysics* 13, 351–359.
- Guzman, A.G., Scheffel, R., Flaherty, S., 2008. The fundamentals of physical characterization of ore for leach. *Hydrometallurgy 2008: Proceedings of the 6th International Symposium, August 18–20, 2008, Phoenix, AZ*, pp. 937–954.
- Hall, C.M., Kesler, S.E., Simon, G., Fortuna, J., 2000. Overlapping Cretaceous and Eocene alteration, Twin Creeks Carlin-type deposit, Nevada. *Economic Geology* 95, 1739–1752.
- Hayley, K., Bentley, L.R., Gharibi, M., Nightingale, M., 2007. Low temperature dependence of electrical resistivity: Implications for near surface geophysical monitoring. *Geophysical Research Letters* 34, L18402.
- Keller, G.V., 1988. Rock and mineral properties. In: Nabighian, M.N. (Ed.), *Electromagnetic methods in applied geophysics: SEG Publ.*, vol. 1, pp. 13–51. Theory, Chap. 2.
- Lefebvre, R., Hockley, D., Smolensky, J., Gelinas, P., 2007. Multiphase transfer processes in waste rock piles producing acid mine drainage. 1: Conceptual model and system characterization. *Journal of Contaminant Hydrology* 52, 137–164.
- Menacho, J.M., Gutierrez, L.E., Chavez, P.A., 2007. Matching theory and practice in heap leaching processes, 6th International Conference COPPER 2007, Toronto, Canada.
- Orr, S., 2002. Enhanced heap leaching – Part 1: insights. *Mining Engineering* 54 (9), 49–56.
- Orr, S., Vesselinov, V., 2002. Enhanced heap leaching – Part 2: applications. *Mining Engineering* 54 (10), 33–38.
- Rucker, D.F., accepted for publication. Moisture estimation within a mine heap: An application of cokriging with assay data and electrical resistivity. *Geophysics*.
- Rucker, D.F., Schindler, A., Levitt, M.T., Glaser, D.R., 2009. Three-dimensional electrical resistivity imaging of a gold heap. *Hydrometallurgy* 98 (3–4), 267–275.
- Schon, J.H., 1996. 1st edition. *Physical properties of rocks, fundamentals and principles of petrophysics*, vol. 18. Pergamon Press.
- Schutz, L., McEvers, L., Saderholm, E., Clarke, L., Trudel, W., Bolin, C.L., 2004. Geologists add value at Newmont's Nevada Mines – part two. *Mining Engineering* 56, 13–22.
- Seal, T., 2004. Enhanced gold extraction in cyanide heap leaching using Hydro-Jex technology. Ph.D. Dissertation, University of Idaho.
- Seal, T., 2007. Hydro-Jex: Heap leach pad stimulation technology; ready for world wide industrial adoption? 2007 SME Annual Meeting February 25–28 Salt Lake City, Utah.
- Seal, T., Jung, S.J., 2005. Reduction of gold inventory in cyanide heap leaching. 2005 SME Annual Meeting: *Got Mining – Preprints*, pp. 163–167.
- Sen, P.N., 1997. Resistivity of partially saturated carbonate rocks with microporosity. *Geophysics* 62, 415–425.
- Simon, G., Kesler, S.E., Chryssoulis, S., 1999. Geochemistry and textures of gold-bearing arsenian pyrite, Twin Creeks, Nevada: Implications for depositions of gold in Carlin-type deposits. *Economic Geology* 94, 405–422.
- Singha, K., Moysey, S., 2006. Accounting for spatially variable resolution in electrical resistivity tomography through field-scale rock physics relations. *Geophysics* 71, A25–A28.
- Taylor, S., Barker, R., 2002. Resistivity of partially saturated Triassic sandstone. *Geophysical Prospecting* 50, 603–613.
- Uhrie, J.L., Koons, G.J., 2001. Evaluation of deeply ripping truck-dumped copper leach stockpiles. *Mining Engineering* 53, 54–56.
- Walker, L.R., Powell, E.A., 2001. Soil water retention on gold mine surfaces in the Mojave Desert. *Restoration Ecology* 9, 95–103.
- Wu, A., Yin, S., Yang, B., Wang, J., Qiu, G., 2007. Study on preferential flow in dump leaching of low-grade ores. *Hydrometallurgy* 87, 124–132.
- Wu, A., Yin, S., Qin, W., Liu, J., Qiu, G., 2009. The effect of preferential flow on extraction and surface morphology of copper sulphides during heap leaching. *Hydrometallurgy* 95, 76–81.